Received: 13 December 2022 | Revised: 19 January 2023 | Accepted: 10 February 2023

DOI: 10.1002/pro.4597

FULL-LENGTH PAPER

THE PROTEIN SOCIETY WILEY

Directed evolution of angiotensin-converting enzyme 2 peptidase activity profiles for therapeutic applications

Pete Heinzelman[1] | **Philip A. Romero**[1,2]

[1]Department of Biochemistry, University of Wisconsin–Madison, Madison, Wisconsin, USA

[2]Department of Chemical & Biological Engineering, University of Wisconsin–Madison, Madison, Wisconsin, USA

Correspondence
Philip A. Romero, 440 Henry Mall, Biochemical Sciences Bldg, Madison, WI 53706, USA.
Email: promero2@wisc.edu

Funding information
US National Institute of Health, Grant/Award Number: 5R35GM119854

Review Editor: Aitziber L. Cortajarena

Abstract

Angiotensin-converting enzyme 2 (ACE2) has been investigated for its ability to beneficially modulate the angiotensin receptor (ATR) therapeutic axis to treat multiple human diseases. Its broad substrate scope and diverse physiological roles, however, limit its potential as a therapeutic agent. In this work, we address this limitation by establishing a yeast display-based liquid chromatography screen that enabled use of directed evolution to discover ACE2 variants that possess both wild-type or greater Ang-II hydrolytic activity and improved specificity toward Ang-II relative to the off-target peptide substrate Apelin-13. To obtain these results, we screened ACE2 active site libraries to reveal three substitution-tolerant positions (M360, T371, and Y510) that can be mutated to enhance ACE2's activity profile and followed up on these hits with focused double mutant libraries to further improve the enzyme. Relative to wild-type ACE2, our top variant (T371L/Y510Ile) displayed a sevenfold increase in Ang-II turnover number (k_{cat}), a sixfold diminished catalytic efficiency (k_{cat}/K_m) on Apelin-13, and an overall decreased activity on other ACE2 substrates that were not directly assayed in the directed evolution screen. At physiologically relevant substrate concentrations, T371L/Y510Ile hydrolyzes as much or more Ang-II than wild-type ACE2 with concomitant Ang-II:Apelin-13 specificity improvements reaching 30-fold. Our efforts have delivered ATR axis-acting therapeutic candidates with relevance to both established and unexplored ACE2 therapeutic applications and provide a foundation for further ACE2 engineering efforts.

KEYWORDS

angiotensin-converting enzyme 2, directed evolution, protein engineering, yeast surface display

1 | INTRODUCTION

Angiotensin-converting enzyme 2 (ACE2) is a zinc-dependent mono-carboxypeptidase found in both membrane bound and freely circulating forms that plays a central role in multiple peptide hormone signaling pathways in humans (Marquez et al., 2021). ACE2 cleaves the terminal phenylalanine residue from

angiotensin-II to produce angiotensin (1–7), resulting in downstream vasodilation and increased salutary blood flow (Shenoy et al., 2011), suppressed inflammation (Hay et al., 2019), and attenuated pathological tissue remodeling after acute injury (Shenoy et al., 2011). These beneficial physiological responses have motivated clinical researchers to pursue ACE2 as an agent for treating respiratory viral infections (Zoufaly et al., 2020), acute respiratory distress syndrome (Khan et al., 2017), and diabetes (Batlle et al., 2012).

While therapeutically administered ACE2 has great potential to modulate the angiotensin-II (Ang-II) axis for treating human disease, this enzyme also acts on at least eight additional peptide hormones found in circulation and/or tissues (Vickers et al., 2002; Zhong et al., 2017). Apelin peptides are major off-target substrates to consider due to their key role in the cardiovascular system, ACE2's high catalytic activity toward multiple Apelin isoforms (Vickers et al., 2002; Wang et al., 2016; Zhong et al., 2017), and the fact that Apelin peptides are found at concentrations 1–2 orders of magnitude higher than Ang-II in human blood and tissues (Chappell, 2016; Sullivan et al., 2015; van Kats et al., 2001; Yavuz & Sevinc, 2015). ACE2-mediated inactivation of Apelins reduces their important cardioprotective effects (Wang et al., 2016) and could trigger myocardial dysfunction when administered therapeutically. ACE2's broad substrate scope and distributed physiological roles greatly limit its potential to specifically cleave Ang-II for therapeutic applications.

In this work, we engineer ACE2 variants with tailored substrate profiles that enable specific cleavage of Ang-II with little or no concomitant effect on off-target peptide signaling pathways such as those involving Apelins. We designed site-directed ACE2 libraries to target key substrate recognition pockets and applied high-performance liquid chromatography (LC)-based screening on mixtures of peptide substrates to mimic heterogeneous in vivo conditions and to identify variants possessing the desired substrate cleavage profiles. After two rounds of directed evolution, we identified ACE2 variants with substantially improved activity and specificity toward Ang-II over Apelin-13. Our leading variant (T371L/Y510Ile) displayed a sevenfold increase in its turnover number (k_{cat}) toward Ang-II and also increased Ang-II:Apelin-13 specificity by up to 30-fold at physiologically relevant substrate concentrations. We also found that our engineered ACE2s display high specificity for Ang-II relative to other peptide hormones that were not directly assayed in our library screening, suggesting a highly focused substrate scope that may allow independent modulation of the Ang-II therapeutic axis. The outcomes presented here will have an important impact on current and future clinical applications of ACE2 for the prevention and treatment of human disease.

2 | RESULTS

2.1 | Yeast surface display-based directed evolution of ACE2 for enhanced activity and specificity

ACE2 acts on different peptide substrates to regulate multiple peptide hormone signaling pathways in vivo (Figure 1a). We sought to engineer ACE2 variants with focused substrate scopes that will allow modulation of Ang-II levels independent of changes in concentrations of other wild-type ACE2 peptide substrates. We developed a streamlined ACE2 screening platform and performed active site-targeted directed evolution to discover new ACE2 variants with enhanced activity and specificity toward Ang-II.

Our ACE2 screening platform leverages yeast surface display (YSD) (Chao et al., 2006; Cherf & Cochran, 2015) to express active ACE2 enzymes on the yeast surface (Figures S1 and S2), allowing subsequent enzyme purification by simple centrifugation and resuspension into assay buffer. We then add individual peptides or mixtures of peptides to the ACE2-expressing yeast and monitor hydrolysis reactions via LC. The combination of yeast display and LC-based screening enables rapid testing of ACE2 variants' substrate hydrolysis profiles.

We tested our yeast display-LC screening platform on Ang-II, angiotensin-I (Ang-I), and Apelin-13 peptide substrates (Figure 1b). We found wild-type ACE2-displaying yeast hydrolyze more than 95% of both Ang-II and Apelin-13 peptides during a 2.5-h room temperature reaction but do not measurably hydrolyze Ang-I. This outcome was expected given that ACE2's catalytic efficiency (k_{cat}/K_m) for Ang-I is nearly 1000-fold lower than those for Ang-II and Apelin-13 (Vickers et al., 2002). We also tested our assay using a mixture of Ang-I, Ang-II, and Apelin-13 peptides to understand ACE2's behavior in a more physiologically relevant substrate environment. We found that Ang-I acts as an inhibitor of ACE2-mediated Ang-II and Apelin-13 hydrolysis under these mixed substrate conditions, with Ang-II and Apelin-13 hydrolysis reduced approximately fivefold.

We next designed site-directed ACE2 libraries to target key residues controlling substrate preference. We examined both the ACE2 crystal structure and a sequence alignment of related peptidases to identify ACE2 residues in the substrate binding pocket that display variation across homologs (Towler et al., 2004; Yan et al., 2020). ACE2's S_1 subsite binds and recognizes the

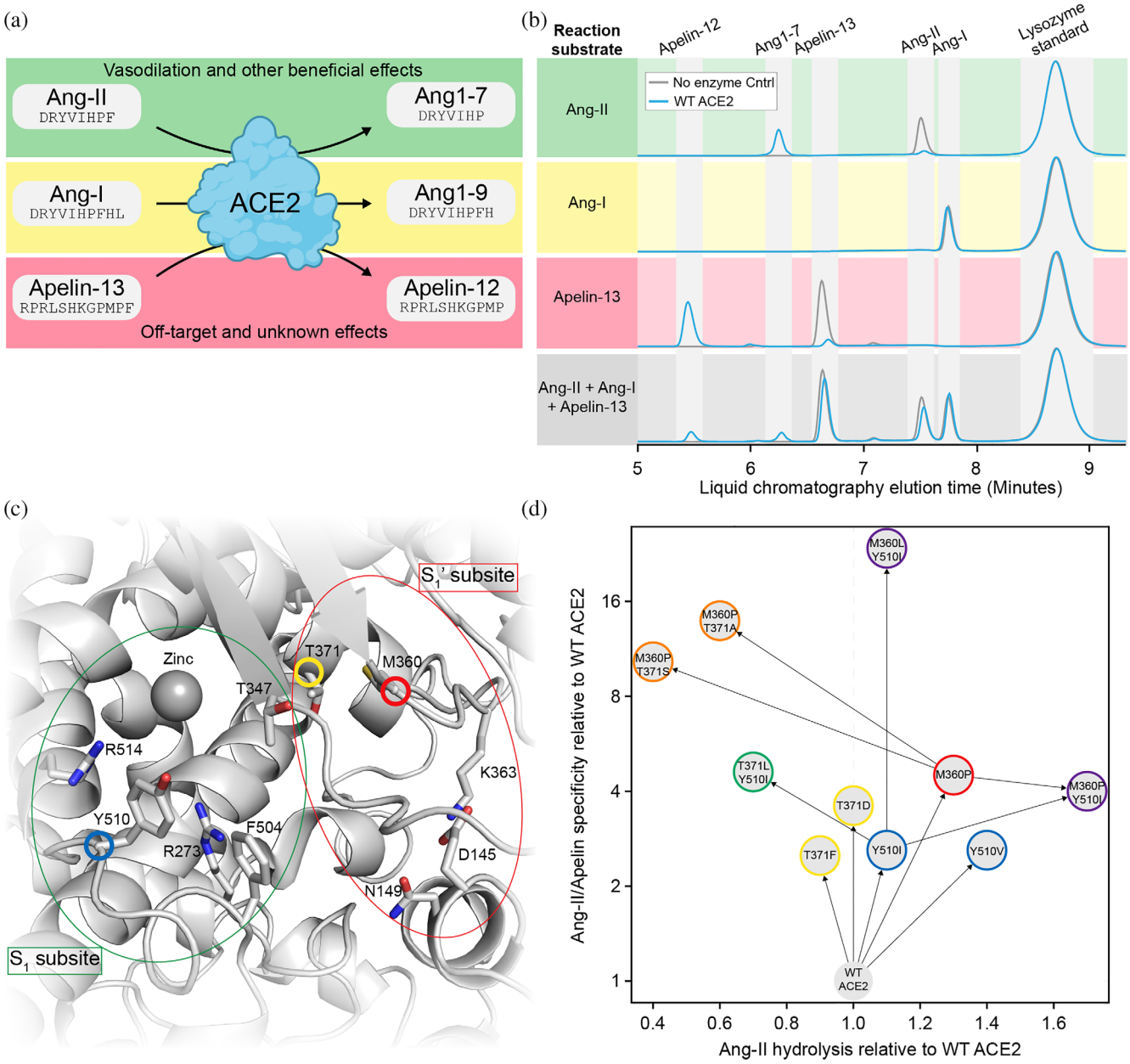

FIGURE 1 Directed evolution of angiotensin-converting enzyme 2 (ACE2) as a therapeutic agent. (a) Key ACE2 peptidase reactions relevant to the Ang-II/ATR therapeutic axis. Green background denotes hydrolysis reaction with beneficial in vivo effects. Red background denotes hydrolysis reaction with detrimental effects. Yellow background indicates unknown and potential for detrimental and/or beneficial, that is, reduction in amount of Ang-I hydrolytic conversion to Ang-II by the ACE dipeptidase, effects. (b) LC chromatograms showing peptide hydrolysis by ACE2-displaying yeast. Our ACE2 system shows high peptidase activity on Ang-II and Apelin-13 substrates, and undetectable hydrolysis of Ang-I. We used horseradish peroxidase-displaying yeast as a negative control. (c) The ACE2 substrate binding pocket is composed of two subsites: S_1 that encases the substrate residue N-terminal to the cleavage site and S_1' that accommodates the final C-terminal residue. The labeled residues correspond to positions for which we constructed and screened yeast-displayed NNB mutant libraries. The three circled residues indicate amino acid positions where mutations enhanced activity and/or specificity. (d) Overview of the directed evolution process. The Ang-II hydrolysis and specificity values were determined using mixed substrate assays from the YSD library screen. Specificity is defined as the ratio of moles Ang-II hydrolysis product to moles Apelin-13 hydrolysis product for the variant ACE2 divided by that same ratio for wild-type ACE2. The numbers reflect single or duplicate measurement from the YSD screen.

main portion of the peptide substrate N-terminal to the cleavage site, while the S_1' site accommodates the C-terminal residue (Figure 1c). We focused on residues R273, F504, Y510, and R514 from the S_1 subsite and residues E145, N149, T347, M360, K363, and T371 from the S_1' subsite. We created 10 individual degenerate NNB

(N denotes all four nucleotides while B denotes C, G, or T) codon libraries at each of these ACE2 positions.

We screened between 5 and 15 clones for each of the 10 site-directed ACE2 libraries using a mixed substrate assay (25 μM Ang-I, 25 μM Ang-II, and 25 μM Apelin-13) to identify variants with improved Ang-II activity and specificity. Given our focus on achieving an initial demonstration of the ability to evolve ACE2 variants with increased activity and/or specificity toward Ang-II, exhaustive screening of these libraries, which would require a considerable amount of time and labor due to the LC screening method's moderate throughput, was not required to realize the goal for this initial ACE2 directed evolution effort. A majority of the sampled clones from the R273, T347, F504, and R514 libraries had diminished Ang-II activity (Table S1), while most of the clones from the E145, N149, and K363 libraries possessed substrate hydrolysis profiles similar to wild-type ACE2. The remaining M360, T371, and Y510 libraries all contained multiple clones with improved Ang-II hydrolysis and Ang-II:Apelin-13 specificity. We identified M360P, T371D, and Y510Ile as the top sampled single mutants at these three sites (Figure 1d).

We next constructed six second-generation libraries using M360P, T371D, and Y510Ile as parents: M360P with NNB at positions 371 or 510, T371D with NNB at 360 or 510, and Y510Ile with NNB at 360 or 371. We screened five randomly sampled clones from each library to assess the relative proportions of functionally impaired and improved variants (Table S2). We found the M360P/T371NNB, Y510Ile/M360NNB, and Y510Ile/T371NNB double mutant libraries warranted further screening by virtue of containing high fractions of active clones. We then screened 18–25 additional clones from these three libraries and identified four leading double mutants: M360P/T371S, M360P/Y510Ile, M360L/Y510Ile, and T371L/Y510Ile (Figure 1d).

2.2 | Engineered ACE2s display enhanced kinetic properties

Our improved ACE2 variants were engineered in a yeast display format where they were fused to cell adhesion proteins on the yeast cell surface. To fully characterize the ACE2 variants' enzymatic activities in a soluble format, which is the format in which they would be administered as therapeutics, we cloned wild-type ACE2 and the leading single and double mutants into a soluble secretion vector (Chan et al., 2020), expressed the enzymes in human embryonic kidney (HEK) cells, and purified the enzymes to greater than 90% homogeneity using Ni-NTA chromatography (Figure S3). Post-purification ACE2 yields were approximately 1 mg/L HEK culture supernatant.

We performed initial enzyme activity assays and found that any variant containing the M360P substitution had undetectable activity when expressed in soluble format (Figure S4). These results indicate that our initial hits containing M360P were dependent on fusion to the yeast surface and that the observed activity profile enhancements cannot be translated to soluble ACE2 enzymes. Given this finding, we did not further pursue any variants containing the M360P substitution.

We performed Michaelis–Menten kinetic studies on wild-type ACE2, Y510Ile, M360L/Y510Ile, and T371L/Y510Ile with the substrates Ang-II, Apelin-13, and Ang-I (Figure 2a). The three engineered variants displayed Ang-II turnover numbers (k_{cat}) at least fourfold greater than wild-type ACE2, but also had increased Michaelis constants (K_m). The T371L/Y510Ile variant showed a 25% increase in Ang-II catalytic efficiency over wild type. In the context of Apelin-13 substrate hydrolysis, the engineered variants showed wild-type-like turnover numbers but also had Michaelis constants that were increased between 5 and 13-fold, resulting in greatly diminished catalytic efficiencies. Wild-type ACE2 and the three variants all hydrolyzed the Ang-I substrate at very slow rates, indicating that the mutations carried by the variants did not increase activity toward Ang-I.

We also evaluated the enzymes' kinetic rates at very low substrate concentrations that reflect the ranges found in human blood and tissues (Chappell, 2016; Sullivan et al., 2015; van Kats et al., 2001; Yavuz & Sevinc, 2015) (Figure 2b). The three engineered variants showed wild-type or near-wild-type Ang-II hydrolysis rates for Ang-II concentrations in the 0.25–1 μM range. The engineered enzymes had almost no activity toward Apelin-13 at substrate concentrations at or below 1 μM and were at least 10-fold less active than wild-type ACE2 in reactions carried out with higher Apelin-13 concentrations. All reaction rates measured on Ang-I were 2–3 orders of magnitude lower than those for Ang-II hydrolysis and are thus too slow to be of physiological relevance.

We evaluated wild-type ACE2's and the engineered variants' substrate hydrolysis rates in reactions containing equimolar mixtures of Ang-II, Apelin-13, and Ang-I to understand substrate preferences and potential interactions between substrates (Figure 2c). Across all mixed substrate concentrations tested, the leading T371L/Y510Ile ACE2 variant has Ang-II hydrolysis activity equal to or greater than wild-type ACE2 and a fivefold or greater decrease in activity toward Apelin-13. Mixed substrate conditions can cause negative interactions between substrates when one substrate acts as an inhibitor for another. As such, we compared results for single and mixed substrate hydrolysis assays and found that the presence of multiple substrates reduces hydrolysis rates for both Ang-II and Apelin-13 (Figure S5). Ang-II

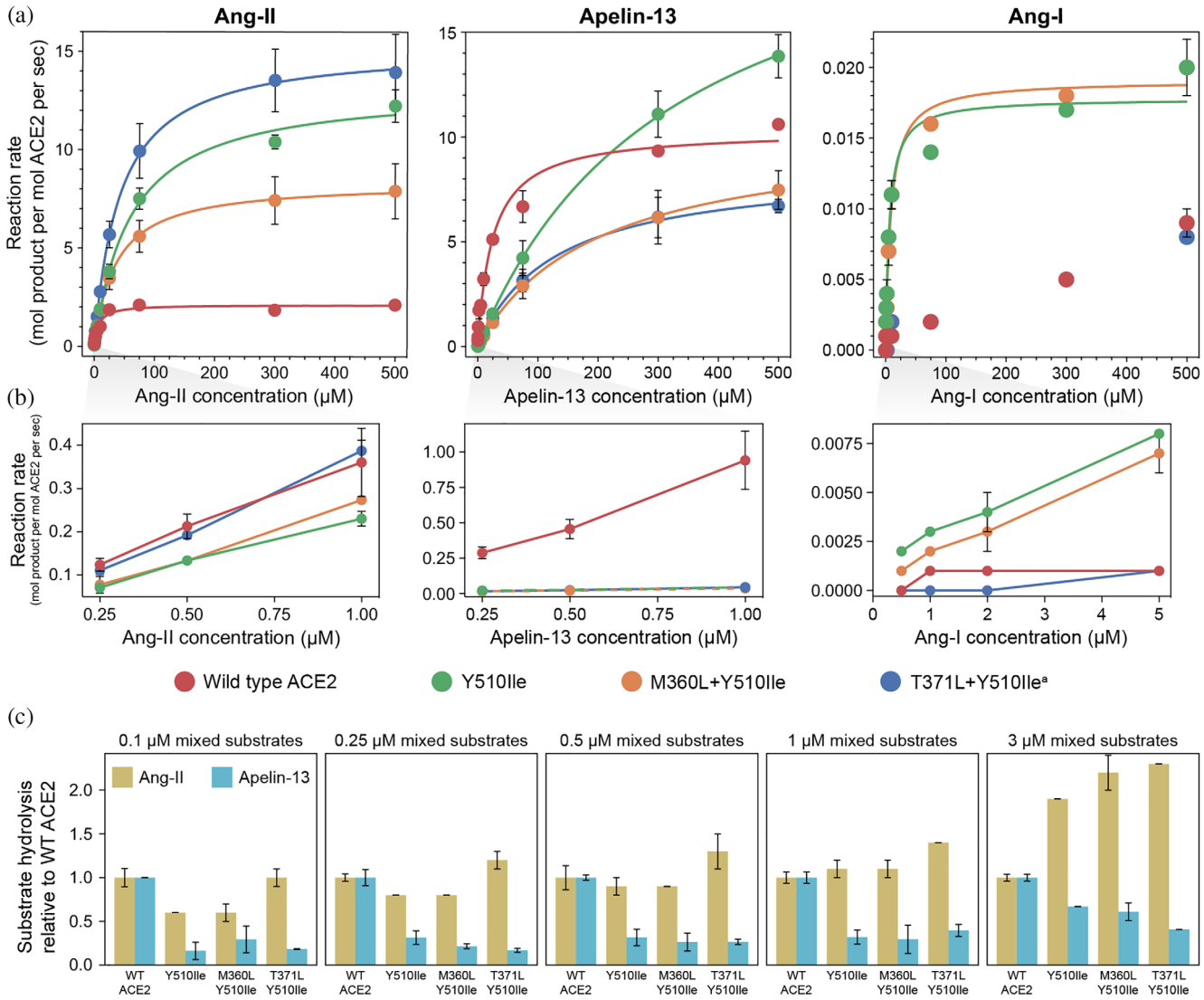

FIGURE 2 Kinetic properties of engineered ACE2 variants. (a) Initial rate plots for single substrate hydrolysis of Ang-II, Apelin-13, and Ang-I peptides. Error bars denote standard deviations for duplicate measurements and the absence of error bars for some data points indicates a standard deviation less than height of data point marker. The lines depict nonlinear regression fits to the Michaelis–Menten equation and the kinetic parameters are reported in Table 1. (b) Initial rate plots zoomed in to lower substrate concentrations that are relevant for physiological functioning in vivo. (c) Relative amounts of Ang-II and Apelin-13 hydrolysis products formed in mixed peptide substrate assays. Ang-I, Ang-II, and Apelin-13 were present at identical concentrations in each reaction and incubated with 250 pM purified ACE2. Activity values are normalized to one for wild-type ACE2. Error bars denote standard deviations (SDs) for duplicate measurements. Error bars for wild-type ACE2 values reflect SD in unnormalized hydrolysis product values for two trials. Error bars for mutant ACE2 values reflect SD in normalized hydrolysis product values. The slow rate of Ang-I hydrolysis relative to Ang-II and Apelin-13 hydrolysis precludes detection of the Ang-I hydrolysis product formation. [a]An additional P235Q mutation was observed in the T371L/Y510Ile variant due to polymerase error during cloning. This mutation is located at a surface position distal to the ACE2 active site and has been found to not affect enzyme activity or specificity.

hydrolysis rates are reduced between two and threefold while Apelin-13 hydrolysis rates are reduced between three and ninefold. Given the results presented in Figure 1b, which indicate that Ang-I inhibits ACE2 hydrolysis of Ang-II and Apelin-13, it appears likely that the presence of Ang-I in the mixed substrate reactions is a substantial contributor to the observed reductions in Ang-II and Apelin-13 hydrolysis rates.

2.3 | Engineered ACE2s retain specificity against other off-target substrates

Given the desire to enhance ACE2's therapeutic utility by narrowing its substrate specificity to enable focused hydrolysis of Ang-II, we were motivated to explore the possibility that evolving ACE2 for increased specificity toward Ang-II relative to

Apelin-13 could simultaneously lead to improvements in specificity relative to other native ACE2 peptide substrates that were not included in the ACE2 mutant library screens. Our finding that all three engineered variants had strongly diminished activity (Figure 3) toward Des-Arg9-bradykinin (dR9-bk), a known ACE2 substrate with sequence RPPGFSPF (Sodhi et al., 2018; Vickers et al., 2002) that was not among the peptides included in library screens, shows that evolving ACE2 for increased specificity relative to one off-target substrate can concomitantly give rise to improvements in specificity relative to other off-target peptides.

To address the possibility that the variants had acquired undesired activity toward nonnative substrates, we measured the activities of these novel enzymes toward Ang1-9, a nonapeptide with sequence DRVYIFPFH that is not hydrolyzed by wild-type ACE2 (Vickers et al., 2002). We found that none of the ACE2 variants exhibited activity toward this peptide in LC assays (Figure S6). Taken with the above observations of mutant ACE2 activities toward Ang-I and dR9-bk, these Ang1-9 hydrolysis assay outcomes suggest that ACE2's activity profile with respect to Ang-II and Apelin-13 hydrolysis can be enhanced without concomitant compromise of specificity toward off-target substrates other than Apelin-13 (Figure 3).

2.4 | Structural rationale for enhanced activity and specificity

We examined the crystal structure of ACE2 (Lubbe et al., 2021) to postulate the mechanisms by which the M360L, T371L, and Y510Ile substitutions influence ACE2's hydrolytic activity and specificity. Y510 resides in the S_1 subsite of ACE2's substrate binding pocket (Figure S7). ACE2 substrates, with the exception of the slowly hydrolyzed Ang-I peptide, feature residues with small sidechains at the P_1 position; both Ang-II and Apelin-13 carry proline at this position.

The Y510Ile substitution increases both k_{cat} and K_m for Ang-II hydrolysis. This coupled increase suggests that the substitution may enlarge the S_1 subsite such that substrate binding is weakened. Reduced binding strength would increase K_m but also increase the energy state of the enzyme-substrate complex and thus reduce the transition state energy barrier (Snider et al., 2004). This reduced energy barrier would be reflected by an increase in k_{cat}. Ang-II and Apelin-13 have the same residues at the P_1 and P_1' positions and thus any specificity differences are likely to be influenced by interactions N-terminal to the P_1 position. Y510Ile's enhanced Ang-II specificity is either a result of direct interactions between Ile510 and these upstream substrate residues or possibly subtle conformational rearrangements that better accommodate the Ang-II substrate.

The sidechains of M360 and T371 line the interior of ACE2's S_1' subsite. This subsite accommodates the C-terminal phenylalanine of both Ang-II and Apelin-13. The similarity in sidechain size among Met, Leu, and Thr suggests that sidechain hydrophobicity, rather than size, at these positions may contribute to the increased Ang-II specificity that arises from the M360L and T371L mutations. Given that Ang-II and Apelin-13 are identical at the P_1 and P_1' positions, there must be some indirect, longer-range effect, either caused by (1) differences in substrate positioning due to substrate residues N-terminal to P_1 or (2) by structural changes induced by substitutions at sites 360/371.

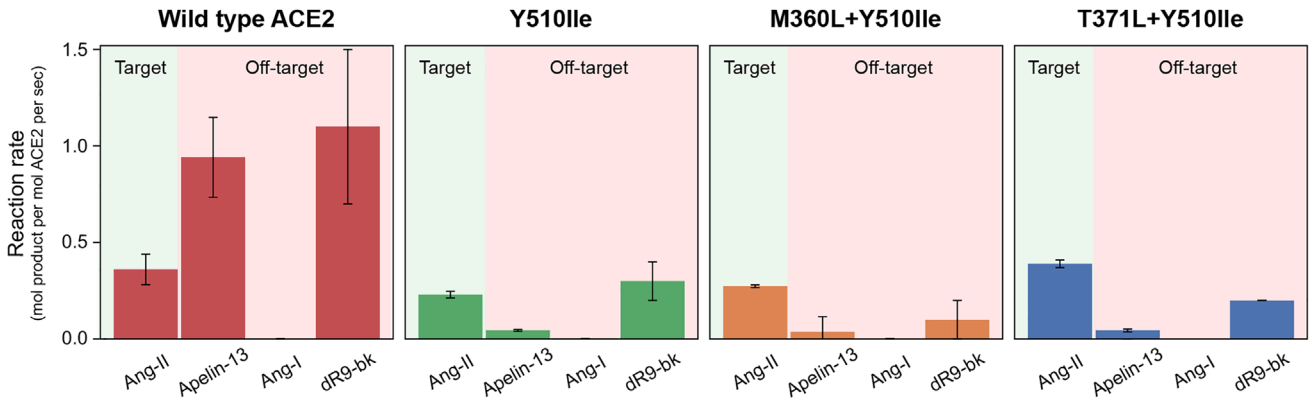

FIGURE 3 Peptide specificity profiles of engineered ACE2 variants. Purified ACE2s were incubated with 1 μM of peptide substrates in single substrate hydrolysis experiments. The engineered variants retain wild-type-like Ang-II hydrolysis, while having substantially reduced activity on Apelin-13 and dR9-bk. Error bars denote standard deviation for duplicate measurements.

3 | DISCUSSION

Although ACE2's ability to regulate Ang-II concentrations in blood and tissues makes the enzyme a candidate for treating a range of diseases, its activity toward numerous other peptides involved in multiple cell signaling pathways limits the degree to which this protein can be utilized in clinical settings. In this work, we sought to augment ACE2's clinical potential by using structure-guided directed evolution as an approach for developing ACE2 variants that hydrolyze Ang-II with high specificity and at high catalytic rates.

Our leading ACE2 variant carried T371L and Y510Ile substitutions that resulted in a sevenfold increase in the Ang-II turnover number (k_{cat}), a sixfold diminished catalytic efficiency (k_{cat}/K_m) on Apelin-13, and an overall decreased activity on other ACE2 substrates that were not directly assayed during the enzyme engineering process. This variant is particularly improved relative to wild-type ACE2 in terms of specificity toward Ang-II relative to Apelin-13; the variant's 25% percent increase in k_{cat}/K_m (Table 1) relative to wild type is modest in comparison to the markedly increased specificity illustrated in Figures 2 and 3. This outcome is unsurprising given that enhancements in enzyme specificity are generally more readily attained than are increases in activity toward native substrates (Bar-Even et al., 2011; Khersonsky et al., 2006). The variant achieved the above desirable functional changes with only two amino acid substitutions, making it nearly identical to wild-type ACE2 and reducing the likelihood that it would induce an undesired immune response when administered as a drug. Taken together, the enzyme enhancements listed above suggest that the T371L/Y510Ile variant would outperform wild-type ACE2 derivatives that have been evaluated in clinical trials.

We developed a YSD-based workflow that enabled streamlined ACE2 variant expression, purification, and screening. This system allowed us to screen 50 ACE2 variants per day with detailed LC-based readouts of substrate hydrolysis profiles. A caveat of this approach is that it assays variants tethered to the yeast cell surface and therefore may identify variants that function only in this context. This caveat is evidenced by our finding that all variants containing the M360P mutation appeared as the top hits in the YSD screen but did not have detectable activity when expressed as soluble enzymes. This loss of hydrolytic activity is not without precedent; display on the yeast surface has been observed to stabilize active conformations of protein mutants that are prone to taking on inactive conformations when free in solution (Burns et al., 2014; Shusta et al., 1999). Given this result with the M360P mutation, there is clearly a need to consider multiple diverse variants when conducting soluble enzyme activity assays to validate YSD screening results. If we had simply chosen the top variants that contained M360P, the desirable effects of the T371L and Y510Ile substitutions in the context of soluble ACE2s would have been masked by the highly deleterious mutation at position 360.

We performed our ACE2 variant screening with a mixture of three ACE2 substrates to enable simultaneous evaluation of enzyme activity and specificity and to engineer ACE2 under conditions that are more representative of the in vivo environment than is the case for screens carried out with a single substrate. In addition to providing this more highly representative substrate environment, the mixed substrate format provides a more

TABLE 1 Ang-II, Apelin-13, and Ang-I hydrolysis kinetic parameters for wild-type and mutant ACE2s.

ACE2	Wild type	Y510Ile	M360L/Y510Ile	T371L/Y510Ile
Ang-II k_{cat} (s^{-1})	2.1 ± 0.2	13.2 ± 0.7	8.4 ± 0.1	15.3 ± 0.3
Ang-II K_m (μM)	7.2 ± 2.8	60.4 ± 10.7	35.9 ± 2.1	42.1 ± 2.5
Ang-II k_{cat}/K_m ($s^{-1} \times M^{-1}$)	2.9×10^5	2.2×10^5	2.3×10^5	3.6×10^5
Apelin-13 k_{cat} (s^{-1})	10.3 ± 1.2	23.1 ± 0.6	10.4 ± 0.3	8.6 ± 0.3
Apelin-13 K_m (μM)	25 ± 10	330 ± 20	200 ± 12	130 ± 15
Apelin-13 k_{cat}/K_m ($s^{-1} \times M^{-1}$)	4.1×10^5	7.0×10^4	5.2×10^4	6.7×10^4
Ang-I k_{cat} (s^{-1})	N/D	0.018 ± 0.02	0.019 ± 0.01	N/D
Ang-I K_m (μM)	N/D	6.4 ± 2.9	8.6 ± 2.5	N/D
Ang-I k_{cat}/K_m ($s^{-1} \times M^{-1}$)	N/D	2.8×10^3	2.2×10^3	N/D

Note: Parameter estimates obtained by using nonlinear fits to initial rate data that appears in Figure 2a. N/D denotes not determined due to the maximum Ang-I concentration assayed (500 μM) being well below the concentration needed to reach the enzyme's maximum hydrolysis rate; this phenomenon precludes accurate kinetic parameter estimation.

stringent screen for ACE2 activity because the presence of multiple substrates reduces the individual reaction rates by several folds (Figure S5). These rate reductions are the result of the mixed substrate conditions causing the ACE2 active site to be occupied by multiple different peptides that each effectively act as competitive inhibitors for the other substrates' hydrolysis reactions. In addition to causing inhibition, the interactions among substrates give rise to subtle shifts in substrate specificity due to the differing k_{cat} and K_m across different substrates. Collectively, the above observations highlight the importance of screening ACE2 variants under mixed substrate conditions.

In this work, we performed an initial shallow screen to show that ACE2 variants with improved activity and specificity can be engineered. A more comprehensive screen of our 10 current ACE2 single site saturation libraries and other site-directed libraries would likely uncover ACE2 variants superior to our leading T371L/Y510Ile double mutant. The best mutant in each NNB site-directed library can be identified 95% of the time by screening only 90 clones (Nov, 2012). Given our LC method's screening capacity of approximately 50 clones per day, 90 clones from all 10 active site saturation mutant libraries could be screened in less than 1 month. The leading single mutants could then be used to design focused double mutant libraries in which one mutation is fixed and a second amino acid position is varied by introduction of a NNB codon. Twenty additional double mutant libraries could be screened with 95% coverage in less than 2 months. These deeper sequence space searches would almost certainly uncover variants that are markedly improved relative to T371L/Y510Ile.

The clinical potential of our engineered ACE2s could be further enhanced by increasing enzyme activity at lower Ang-II concentrations and directly screening against known off-target ACE2 substrates including des-Arg9-bradykinin and Dynorphin-A. Mutants arising from such additional engineering efforts could be characterized in pharmacokinetics, biodistribution, toxicity, and pharmacodynamics studies with wild-type mice. This initial in vivo ACE2 variant profiling would provide a foundation for follow-on studies with mouse models of specific diseases and subsequent advancement to human trials.

Our directed evolution method has enabled isolation of ACE2 variants with potential to outperform wild-type ACE2 as protein therapeutics. This outcome is important for advancing current ACE2 therapeutic applications, such as treating respiratory distress associated with traumatic injuries or viral infection (Zoufaly et al., 2020), and giving rise to new ACE2 biomedical uses including Alzheimer's disease therapy (Evans et al., 2020). Furthermore, these results provide a foundation for developing additional directed evolution methods, such as microfluidics droplet-based screening to augment ACE2 activity and specificity (Holstein et al., 2021), that facilitate sampling larger swaths of ACE2 sequence space and thus further enable ACE2 to realize its potential as an agent for treating and preventing a wide range of health conditions.

4 | MATERIALS AND METHODS

4.1 | ACE2 library generation and screening

Residues 18–615 of the human (UniProt Q9BYF1) ACE2 gene was synthesized as a yeast codon-optimized gBlock (Integrated DNA Technologies, Coralville, IA) and ligated into the yeast display vector VLRB.2D-aga2 (provided by Dane Wittrup, MIT); this vector fuses the aga2 protein to the C-terminus of ACE2 (Figure S1). Site-directed mutant libraries were constructed via overlap extension PCR. Oligonucleotide primers carrying NNB base triplets were purchased from Integrated DNA Technologies. The degenerate "B" base is comprised of a mixture of C, G, and T bases while the degenerate "N" base is composed of all four nucleotide bases. Primers CDspLt (5′-GTCTTGTTGGCTATCTTCGCTG-3′) and CDspRt (5′-GTCGTTGACAAAGAGTACG-3′) were used as outer primers for ACE2 gene amplification reactions. Overlap extension PCR products were digested and ligated into the YSD vector. Total colony counts for each single site-directed mutant library ranged from 500 to 2000.

DNA was harvested from *Escherichia coli* cultures and transformed into the EBY100 YSD strain (Chao et al., 2006) that had been made chemically competent using the Frozen EZ-Yeast Transformation II Kit (Zymo Research). Individual yeast colonies were picked into 4 mL of pH 4.5 Sabouraud Dextrose Casamino Acid media (SDCAA: components per liter—20 g dextrose, 6.7 g yeast nitrogen base [VWR Scientific, Radnor, PA], 5 g Casamino Acids [VWR], 10.4 g sodium citrate, and 7.4 g citric acid monohydrate) and grown overnight at 30°C and 250 rpm. For induction of ACE2 display, a 5 mL pH 7.4 SGCAA (components per liter—8.6 g $NaH_2PO \times H_2O$, 5.4 g Na_2HPO_4, 20 g galactose, 6.7 g yeast nitrogen base, and 5 g Casamino Acids) culture was started at an optical density, as measured at 600 nm, of 0.5 and shaken overnight at 250 rpm and 20°C.

For LC determination of yeast-displayed ACE2 peptidase activity ~0.05 OD × mL of induced yeast were resuspended in 400 μL of ACE2 reaction buffer (50 mM 2-[N-morpholino]ethanesulfonic acid [MES], 300 mM

NaCl, 10 μM $ZnCl_2$, 0.02% w/v Hen Egg Lysozyme [Sigma-Aldrich, St. Louis, MO] as carrier protein, pH 6.5) containing 25 μM each angiotensin-I (Anaspec, Fremont, CA), angiotensin-II (Anaspec), and Apelin-13 (Bachem, Torrance, CA) and tumbled in microfuge tubes at room temperature for 2.5 h. Reactions were centrifuged to pellet yeast and supernatants withdrawn for LC analysis.

LC analyses were performed on a Shimadzu 2020 LC–MS. Reaction supernatants were injected onto a 3 × 150 mm, 100 Å, 5 μm Polar C18 Luna Omega column (Phenomenex, Torrance, CA). Mobile phase A consisted of 0.02% (v/v) trifluoroacetic acid in water, and mobile phase B consisted of 0.016% (v/v) trifluoroacetic acid in acetonitrile. Area under the LC chromatogram curve, that is, UV detector millivolts multiplied by elution timespan in seconds, was used as the metric for amount of product formed during the hydrolysis reaction.

For construction of ACE2 double mutant libraries that used leading single mutant clones, that is, clone 360-7, 371-11, and 510-11 as described in Section 2, plasmids were rescued from yeast liquid culture using the Zymo Research Yeast Plasmid Miniprep II Kit. Rescued plasmids were used as templates for overlap PCR reactions carried out to introduce NNB codons, at the positions noted in Section 2, into the three respective single mutant ACE2 parent genes. Double mutant library plasmid construction and yeast transformation were carried out as described above for site-directed ACE2 single mutant libraries. Sequences for leading ACE2 double mutants were obtained by rescuing plasmids, amplifying mutant ACE2 genes using primers CDspLt and CDspRt, and sequencing the PCR products using primers CDspLt, CDspRt, and SqHmFw (5′-GGACTTTCAGGAAGACAACG-3′).

4.2 | Soluble expression and purification of wild type and ACE2 variants

Plasmid pcDNA3-sACE2(WT)-8his (Chan et al., 2020), which encodes human ACE2 residues 1–615 with native human codon representation and appends the gene with a C-terminal His_8 tag, was used as template for creation of ACE2 genes carrying hydrolysis profile-modifying mutations identified during yeast displayed-ACE2 library screening. Mutant genes were constructed by overlap extension PCR using outer primers SqLtPck (5′-CGTGGATAGCGGTTTGACTCAC-3′) and PckRvSq (5′-CCTACTCAGACAATGCGATGC-3′), and ligated into pcDNA3-sACE2(WT)-8his. Mutant ACE2 gene sequences were verified using primers SqLtPck, PckRvSq, and PckF260 (5′-GTTACTGATGCAATGGTGGACC-3′).

HEK 293T cells (Product #CRL-3216, ATCC, Manassas, VA) were grown in DMEM (ATCC) supplemented with 10% fetal bovine serum (FBS), 2 mM L-glutamate (Invitrogen, Carlsbad, CA), and 1× penicillin–streptomycin (Invitrogen). Cells were transfected with ACE2 expression plasmid DNA using jetPRIME transfection reagent (PolyPlus, Illkirch-Graffenstaden, France). Following the 4-h transfection interval DMEM containing DNA and transfection reagent was replaced with 10 mL of OptiMEM (Invitrogen) supplemented with 1× Pen–Strep and ACE2 expression was allowed to proceed for 40–48 h.

Culture supernatants were syringe filtered using 0.22 μm polyethersulfone (PES) Whatman PuraDisc filters (Cytiva, Marlborough, MA) with concentration and buffer exchange into pH 7.4 PBS subsequently performed using 30-kDa MWCO VivaSpin20 centrifugal concentrator units (Cytiva). His_8-tagged ACE2 proteins were purified from buffer-exchanged supernatants using Qiagen Ni-NTA resin. Purified ACE2 proteins were buffer exchanged into 25 mM Tris–HCl, pH 7.5 containing 10 μM $ZnCl_2$ using Zeba Spin desalting columns (Fisher Scientific, Waltham, MA) and protein concentrations determined using the Pierce Coomassie Protein Assay kit (Fisher Scientific).

4.3 | Activity and specificity profiling of purified ACE2 proteins

Peptide substrate hydrolysis assays were carried out at room temperature and 150 μL scale in 96-well plates using 50 mM MES, 300 mM NaCl, 10 μM $ZnCl_2$, 0.01% (v/v) Brij-35 (Sigma-Aldrich) as reaction buffer. Reactions were halted by addition of 1M EDTA solution, pH 8, after intervals, which ranged from 3 min to 2.5 h, during which less than 15% of the input peptide substrate had been hydrolyzed. ACE2 concentrations added to assays for the various peptide substrates evaluated were as follows: Ang-I/1.75 nM, Ang-II/700 pM, Apelin-13/1.4 nM, des-Arg9-bradykinin/700 pM, Ang (1–9)/700 pM, Multiplex/250 pM. Des-Arg9-bradykinin and Ang1-9 were purchased from Anaspec and ApexBio (Houston, TX) respectively.

Moles of product formed in hydrolysis reactions used for ACE2 activity and specificity quantification was determined by comparing area under the curve for LC chromatograms to chromatogram areas in which >95% input substrate conversion was achieved by incubation of substrate with 25 nM recombinant human ACE2 commercial standard (BioLegend, San Diego, CA) for between 1 and 4 h pending substrate used. Kinetic parameters for Ang-I, Ang-II, and Apelin-13 hydrolysis were determined

by fitting initial rates data using GraphPad Prism software (GraphPad, San Diego, CA).

AUTHOR CONTRIBUTIONS

Philip A. Romero: Conceptualization (equal); funding acquisition (equal); project administration (lead); supervision (equal); writing – original draft (equal). **Pete Heinzelman:** Conceptualization (equal); investigation (lead); methodology (lead); writing – original draft (equal); writing – review and editing (equal).

ACKNOWLEDGMENTS

This work was supported by the US National Institutes of Health (5R35GM119854). "The content is solely the responsibility of the authors and does not necessarily represent the official views of the National Institutes of Health."

DATA AVAILABILITY STATEMENT

The data that support the findings of this study are available from the corresponding author upon reasonable request.

ORCID

Pete Heinzelman https://orcid.org/0000-0002-5588-3731

REFERENCES

Bar-Even A, Noor E, Savir Y, Liebermeister W, Davidi D, Tawfik DS, et al. The moderately efficient enzyme: evolutionary and physicochemical trends shaping enzyme parameters. Biochemistry. 2011;50(21):4402–10.

Batlle D, Wysocki J, Soler MJ, Ranganath K. Angiotensin-converting enzyme 2: enhancing the degradation of angiotensin II as a potential therapy for diabetic nephropathy. Kidney Int. 2012;81(6):520–8.

Burns ML, Malott TM, Metcalf KJ, Hackel BJ, Chan JR, Shusta EV. Directed evolution of brain-derived neurotrophic factor for improved folding and expression in *Saccharomyces cerevisiae*. Appl Environ Microbiol. 2014;80(18):5732–42.

Chan KK, Dorosky D, Sharma P, Abbasi SA, Dye JM, Kranz DM, et al. Engineering human ACE2 to optimize binding to the spike protein of SARS coronavirus 2. Science. 2020;69(6508):1261–5.

Chao G, Lau WL, Hackel BJ, Sazinsky SL, Lippow SM, Wittrup KD. Isolating and engineering human antibodies using yeast surface display. Nat Protoc. 2006;1(2):755–68.

Chappell MC. Biochemical evaluation of the renin-angiotensin system: the good, bad, and absolute? Am J Physiol Heart Circ Physiol. 2016;310(2):H137–52.

Cherf GM, Cochran JR. Applications of yeast surface display for protein engineering. Methods Mol Biol. 2015;1319:155–75.

Evans CE, Miners JS, Piva G, Willis CL, Heard DM, Kidd EJ, et al. ACE2 activation protects against cognitive decline and reduces amyloid pathology in the Tg2576 mouse model of Alzheimer's disease. Acta Neuropathol. 2020;139(3):485–502.

Hay M, Polt R, Heien ML, Vanderah TW, Largent-Milnes TM, Rodgers K, et al. A novel angiotensin-(1-7) glycosylated Mas receptor agonist for treating vascular cognitive impairment and inflammation-related memory dysfunction. J Pharmacol Exp Ther. 2019;369(1):9–25.

Holstein JM, Gylstorff C, Hollfelder F. Cell-free directed evolution of a protease in microdroplets at ultrahigh throughput. ACS Synth Biol. 2021;10(2):252–7.

Khan A, Benthin C, Zeno B, Albertson TE, Boyd J, Christie JD, et al. A pilot clinical trial of recombinant human angiotensin-converting enzyme 2 in acute respiratory distress syndrome. Crit Care. 2017;21(1):234.

Khersonsky O, Roodveldt C, Tawfik DS. Enzyme promiscuity: evolutionary and mechanistic aspects. Curr Opin Chem Biol. 2006;10(5):498–508.

Lubbe L, Cozier GE, Oosthuizen D, Acharya KR, Sturrock ED. ACE2 and ACE: structure-based insights into mechanism, regulation and receptor recognition by SARS-CoV. Clin Sci (Lond). 2021;134(21):2851–71.

Marquez A, Wysocki J, Pandit J, Batlle D. An update on ACE2 amplification and its therapeutic potential. Acta Physiol (Oxf). 2021;231(1):e13513.

Nov Y. When second best is good enough: another probabilistic look at saturation mutagenesis. Appl Environ Microbiol. 2012;78(1):258–62.

Shenoy V, Qi Y, Katovich MJ, Raizada MK. ACE2, a promising therapeutic target for pulmonary hypertension. Curr Opin Pharmacol. 2011;11(2):150–5.

Shusta EV, Kieke MC, Parke E, Kranz DM, Wittrup KD. Yeast polypeptide fusion surface display levels predict thermal stability and soluble secretion efficiency. J Mol Biol. 1999;292(5):949–56.

Snider M, Temple B, Wolfenden R, Snider MG, Temple BS, Wolfenden R. The path to the transition state in enzyme reactions: a survey of catalytic efficiencies. J Phys Org Chem. 2004;17(6–7):586–91.

Sodhi CP, Wohlford-Lenane C, Yamaguchi Y, Prindle T, Fulton WB, Wang S, et al. Attenuation of pulmonary ACE2 activity impairs inactivation of des-Arg9 bradykinin/BKB1R axis and facilitates LPS-induced neutrophil infiltration. Am J Physiol Lung Cell Mol Physiol. 2018;314(1):L17–31.

Sullivan JC, Rodriguez-Miguelez P, Zimmerman MA, Harris RA. Differences in angiotensin (1-7) between men and women. Am J Physiol Heart Circ Physiol. 2015;308(9):H1171–6.

Towler P, Staker B, Prasad SG, Menon S, Tang J, Parsons T, et al. ACE2 X-ray structures reveal a large hinge-bending motion important for inhibitor binding and catalysis. J Biol Chem. 2004;279(17):17996–8007.

van Kats JP, Schalekamp MADH, Verdouw PD, Duncker DJ, Danser AHJ. Intrarenal angiotensin II: interstitial and cellular levels and site of production. Kidney Int. 2001;60(6):2311–7.

Vickers C, Hales P, Kaushik V, Dick L, Gavin J, Tang J, et al. Hydrolysis of biological peptides by human angiotensin-converting enzyme-related carboxypeptidase. J Biol Chem. 2002;277(17):14838–43.

Wang W, McKinnie SMK, Farhan M, Paul M, McDonald T, McLean B, et al. Angiotensin-converting enzyme 2 metabolizes and partially inactivates Pyr-Apelin-13 and Apelin-17: physiological effects in the cardiovascular system. Hypertension. 2016;68(2):365–77.

Yan R, Zhang Y, Li Y, Xia L, Guo Y, Zhou Q. Structural basis for the recognition of SARS-CoV-2 by full-length human ACE2. Science. 2020;367(6485):1444–8.

Yavuz YC, Sevinc C. Role of circulating serum Apelin-13 levels in glomerulonephritis: a pilot study. J Clin Exp Nephrol. 2015;1:2. https://doi.org/10.21767/2472-5056.100002

Zhong JC, Zhang ZZ, Wang W, McKinnie SMK, Vederas JC, Oudit GY. Targeting the apelin pathway as a novel therapeutic approach for cardiovascular diseases. Biochim Biophys Acta Mol Basis Dis. 2017;1863(8):1942–50.

Zoufaly A, Poglitsch M, Aberle JH, Hoepler W, Seitz T, Traugott M, et al. Human recombinant soluble ACE2 in severe COVID-19. Lancet Respir Med. 2020;8(11):1154–8.

SUPPORTING INFORMATION

Additional supporting information can be found online in the Supporting Information section at the end of this article.

How to cite this article: Heinzelman P, Romero PA. Directed evolution of angiotensin-converting enzyme 2 peptidase activity profiles for therapeutic applications. Protein Science. 2023; 32(4):e4597. https://doi.org/10.1002/pro.4597